

# Numerical analysis of Hypersonic Combustion of a Scramjet Combustor with a Central lobed Strut Injector at Flight Mach Number 7

K.M Pandey, Gautam Choubey

**Abstract**— A numerical study of the inlet-combustor interaction and flow structure through a scramjet engine at a flight Mach number  $M = 7$  (Hypersonic Combustion) is presented. The scramjet configuration incorporates an inlet with an 8 degree compression ramp, followed by an isolator, and a divergent combustor. Fuel is injected at supersonic speed ( $M=2$ ) through a central strut injector. The shape of the strut is chosen in a way to produce strong stream wise vorticity and thus to enhance the hydrogen/air mixing. To investigate the influence of the central injector on the flow behavior, reacting cases have been studied. For the reacting cases, the shock wave pattern is modified due to the strong heat release during combustion process. The shock structure and combustion phenomenon are not only affected by the geometry, but also by the flight Mach number and the trajectory. The  $k-\epsilon$  realizable computations are capable of predicting mixing and combustion simulations well and good. For all reacting cases, fuel-air stoichiometric conditions are used.

**Index Terms**— Scramjet, Hypersonic Combustion,  $k-\epsilon$  realizable model, Flameholder.

## I. INTRODUCTION

Hydrogen-fueled scramjet engines will play a very important role in the future access to space and hypersonic flight programs. Scramjet Powered vehicles are able to increase the payload significantly in comparison with traditional rocket powered vehicles. In the field of hypersonic propulsion, the Research Training Group GRK 1095 "Aero-thermodynamic Design of a Scramjet Propulsion System" is focused on the scramjet technology involving highly interdisciplinary numerical and experimental studies to design and develop a scramjet demonstrator.<sup>20, 21</sup> Within the framework of the GRK 1095, several experiments at ground conditions have been performed in the supersonic combustion test facility at the Institute of Aerospace Thermodynamics (ITLR). The second phase of the GRK 1095 program is focused on the design of a scramjet demonstrator for flight conditions at Mach number of 8 and at an altitude of 30 km.

For a number of reasons, hydrogen is often considered as the fuel for scramjets for hypersonic vehicles. Information on delay periods for hydrogen-air systems is not plentiful.

Although static temperatures and Pressures can, to a certain extent, be controlled by intake design, an accurate knowledge of the dependence of delay period on these and the equivalence ratio is mandatory before a proper balance can be drawn among all the design considerations. An experimental investigation would be the most satisfactory way to resolve the problem. Such an investigation, however, would have been both expensive and technically difficult.

In the present study, the full integration of the inlet, isolator and combustor was investigated. A numerical investigation of the inlet-combustor interaction and flow structure through the supersonic combustor is presented. Different parameters are studied, like wall pressure, density, temperature and Mach number distribution. For the purpose of validation, the  $k-\epsilon$  realizable results are compared with experimental data for static pressure at the top wall. In addition, qualitative comparisons are also made between predicted and measured shadowgraph images. The  $k-\epsilon$  realizable computations are capable of predicting flow simulations well and good.

## II. LITERATURE REVIEW

E. Rabadan, B. Weigand. [1] worked on the topic "Numerical Investigation of a Hydrogen-fueled Scramjet Combustor at Flight Conditions" and their findings are- As the equivalence ratio was increased, the combustion became stronger causing an upstream displacement of the shock train producing different pressure variations. T. Nguyen [2] worked on the topic "Numerical Investigations of Relaminarization in Supersonic and Hypersonic Flows" and their findings are- In the vicinity downstream of the expansion corner, the pressure and the wall shear stress are reduced and the boundary layer is fuller and thicker. Vadim Yu. Aleksandrov Alexander N. Prokhorov Vyacheslav L. Semenov [3] worked on "Hypersonic Technology Development Concerning High Speed Air-Breathing Engines" and they found that small penetration of fuel into supersonic flow causes combustion only near to a wall, large losses of total pressure. K. A. Skinner and R. J. Stalker [4] worked on "Species Measurements in a Hypersonic, Hydrogen-Air, and Combustion Wake" and found that at lower pressures, the ignition delay and heat release times will be much greater than the minimum values of 0.5 and 1 ms respectively. J. Swithenbank [5] worked on "Hypersonic Air-breathing propulsion" and his findings are chemical rearrangement time for combustion can be large at low temperature and pressures. I. N. Momtchiloff, E. D. Taback, and R. F. Buswell [6] worked on "Kinetics in Hydrogen-Air flow systems. I. Calculations of ignition delays for hypersonic ramjets and their findings are- The ignition delay length

Manuscript received February, 2014.

Dr.K.M Pandey Department of Mechanical Engineering, NIT Silchar, Assam, India.

Gautam Choubey, M.Tech-, Thermal Engineering, Department of Mechanical Engineering, N.I.T Silchar, Assam, India.

increases rapidly at the lower flight Mach numbers. Richard C. Oldenborg, David M. Harradine, Gary W. Loge, John L. Lyman, Garry L. Schott. And Kenneth R. Winn [7] worked on “Critical Reaction rates in Hypersonic Combustion Chemistry” and found that High Mach number flight also results in very short residence times (millisecond time range) in a hypersonic engine which causes poor chemical combustion efficiency. S. Yungster, K. Radhakrishnan [8] worked on “Simulation of unsteady hypersonic combustion around projectiles in an expansion tube” and found that the flame propagation produces a series of oblique shock waves that reignite the core flow, creating an oblique detonation wave whose interaction with the laterally expanding boundary layer flame gives rise to a normal detonation wave that propagates. K. Kumaran and V. Babu [9] worked on “Investigation of the effect of chemistry models on the numerical predictions of the supersonic combustion of Hydrogen.” And their findings are-Multi step chemistry predicts higher and wider spread heat release than what is predicted by single step chemistry. Shigeru Aso et.al [10] worked on “Fundamental study of supersonic combustion in pure air flow with use of shock tunnel” and found that the increase of injection pressure generated strong bow shock, resulting in the pressure losses. The shock generator is an effective method to accelerate the combustion.

S. Zakrzewski and Milton [11] carried out an experiment on “Supersonic liquid fuel jets injected into quiescent air”. They found that Supersonic liquid jets  $M = 1.8$  develops from a flat front to a rounded bow within some 10 mm  $M = 5.2$ , the bow shape is more pointed and shows signs of an oscillation from more to less pointed. Kyung Moo Kim et.al [12] presented Numerical study on supersonic combustion with cavity-based fuel injection and found when the wall angle of cavity increases, the combustion efficiency is improved, but total pressure loss increased.

D. Cecere, A. Ingenito [13] worked on Hydrogen/air supersonic combustion for future Hypersonic vehicles and their findings are-The heat released and the fast hydrogen jets produces 3-D large structures and large vorticity rates, therefore enhancing turbulent mixing. Ghislain Tchuen [14] worked on the topic Numerical study of the interaction of type IVr around a double-wedge in hypersonic flow and found that Real gas effects significantly change the flow field behind the shock wave. M Deepu [15] carried out Recent Advances in Experimental and Numerical Analysis of Scramjet Combustor Flow Fields and found that Increase in jet to free stream momentum flux ratio will result in the increase of jet penetration to free stream for all kinds of jets..

### III. GOVERNING EQUATIONS

The advantage of employing the complete Navier-Stokes equations extends not only to the investigations that can be carried out on a wide range of flight conditions and geometries, but also in the process the location of shock wave, as well as the physical characteristics of the shock layer, can be precisely determined. We begin by describing the three-dimensional forms of the Navier-Stokes equations below. Neglecting the presence of body forces and volumetric heating, the three-dimensional Navier-Stokes equations are derived as

Continuity:

$$\frac{\partial \rho}{\partial t} + \frac{\partial(\rho u)}{\partial x} + \frac{\partial(\rho v)}{\partial y} + \frac{\partial(\rho w)}{\partial z} = 0 \quad \text{----- (1)}$$

X momentum:

$$\frac{\partial(\rho u)}{\partial t} + \frac{\partial(\rho uu)}{\partial x} + \frac{\partial(\rho uv)}{\partial y} + \frac{\partial(\rho uw)}{\partial z} = \frac{\partial \sigma_{xx}}{\partial x} + \frac{\partial \tau_{yx}}{\partial y} + \frac{\partial \tau_{zx}}{\partial z} \quad \text{----- (2)}$$

Y momentum:

$$\frac{\partial(\rho v)}{\partial t} + \frac{\partial(\rho uv)}{\partial x} + \frac{\partial(\rho vv)}{\partial y} + \frac{\partial(\rho vw)}{\partial z} = \frac{\partial \tau_{xy}}{\partial x} + \frac{\partial \sigma_{yy}}{\partial y} + \frac{\partial \tau_{zy}}{\partial z} \quad \text{----- (3)}$$

Z momentum:

$$\frac{\partial(\rho w)}{\partial t} + \frac{\partial(\rho uw)}{\partial x} + \frac{\partial(\rho vw)}{\partial y} + \frac{\partial(\rho ww)}{\partial z} = \frac{\partial \tau_{xz}}{\partial x} + \frac{\partial \tau_{yz}}{\partial y} + \frac{\partial \sigma_{zz}}{\partial z} \quad \text{----- (4)}$$

Energy:

$$\frac{\partial(\rho E)}{\partial t} + \frac{\partial(\rho uE)}{\partial x} + \frac{\partial(\rho vE)}{\partial y} + \frac{\partial(\rho wE)}{\partial z} = \frac{\partial(u\sigma_{xx} + v\tau_{xy} + w\tau_{xz})}{\partial x} + \frac{\partial(u\tau_{yx} + v\sigma_{yy} + w\tau_{zy})}{\partial y} + \frac{\partial(u\tau_{xz} + v\tau_{yz} + w\sigma_{zz})}{\partial z} + \frac{\partial(K\frac{\partial T}{\partial x})}{\partial x} + \frac{\partial(K\frac{\partial T}{\partial y})}{\partial y} + \frac{\partial(K\frac{\partial T}{\partial z})}{\partial z} \quad \text{--- (5)}$$

### IV. THE SCRAMJET COMBUSTOR

The scramjet demonstrator consists of an intake with a compression ramp and sidewalls, followed by an isolator, a combustor and a nozzle (Fig. 3.1). The compression ramp has a total length of 487mm with an angle of 8 degree. In the inlet section, the compression ramp covers 272mm and it continues 214mm downstream under the cowl. The isolator section starts after the inlet, and it extends to the combustor section in the form of a divergent duct with variable cross section area. The length of the scramjet (inlet, isolator and combustor) is 1550mm with a constant cross-section width of 65mm and maximum height of 71 mm. The scramjet nozzle is formed by the external geometry of the airframe demonstrator.

For the present numerical study, the coupling of the inlet, isolator and combustor components is referred as the scramjet. The central strut injector is located at axial position  $x = 650$  mm. The general dimensions are: 86mm in length, 65mm in width and 7mm in height. The strut injector has 7 horizontal and 6 vertical injection ports located at the trailing edge. The area of each horizontal and vertical port is  $5.25\text{mm}^2$  and  $1.20\text{mm}^2$ , respectively (Fig. 2). Hydrogen is injected parallel to the flow and mixed downstream by means of strong stream wise vortices produced by the geometry of the lobed strut injector. The inflow conditions for all simulations correspond to the flight design point (Mach number  $M = 8$ , altitude  $h = 30$  km) showed in table 1. For all simulations, wall temperatures were set to  $T_{wall} = 900\text{K}$  since wall cooling is expected in a real flight.

For the reacting case, hydrogen was injected at the static temperature of  $T_{H_2} = 300K$  with a Mach number of  $M = 2$ . For the reacting cases, a stoichiometric condition was used.

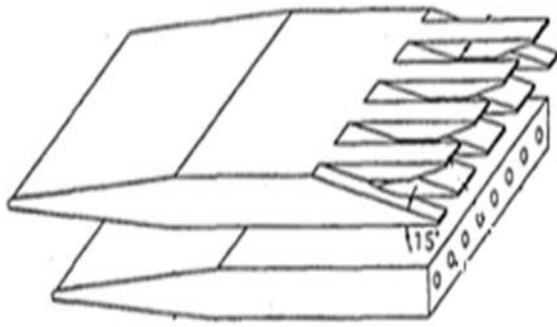


Fig. 1: Central lobed strut injector



Fig.2: Scramjet Hypersonic test model

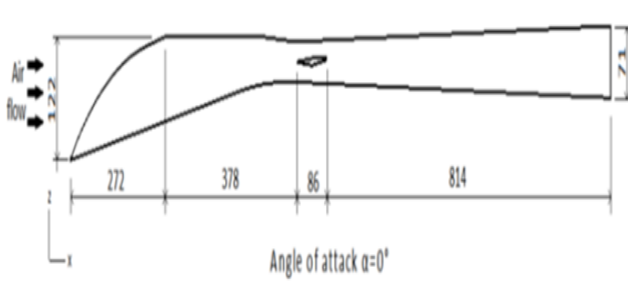


Fig. 3: General dimensions of the inlet-combustor configuration with central strut injector (all dimensions are in mm). Angle of attack  $\alpha = 0^\circ$  is defined with the parallel position of the central injector with respect to the incoming free stream flow.

### V. BOUNDARY CONDITIONS

Three types of boundaries are applied: inflow, outflow and fixed walls and the entire flow field is considered to be supersonic. Dirichlet boundary conditions are applied for variables at inflow and Neumann boundary conditions are used for all variables at outflow. Also no slip condition is applied on fixed walls. The computations are all initialized with the state of incoming air.

Table No: 1

S.No	Variables	Air	Hydrogen
1	Ma	7	2
2	T(k)	520.92	300
3	P(Pa)	1940.28	101325
4	$m^\circ(Kg/s)$	0.85	0.027
5	$K(m^2/s^2)$	10	2400
6	$\epsilon (m^2/s^3)$	650	1e+08
7	$Y_{O_2}$	0.232	0
8	$Y_{N_2}$	0.736	0
9	$Y_{H_2O}$	0.032	0
10	$Y_{H_2}$	0	1

### VI. RESULTS AND DISCUSSIONS

In this section we describe the results from the numerical simulations for strut with central lobed injector for reacting (Mixing case) only.

Fig.4 shows a view of the flow together with a qualitative comparison of experimental shadowgraph images and numerical images from the cases of  $H_2$  injection. With  $H_2$  injection, oblique shocks are formed at the tip of the wedge that is later reflected by the upper and lower walls. At the upper and lower walls, the boundary layer is affected by the reflected oblique shocks. In some places the reflected shock waves are deflected by the hydrogen jets.

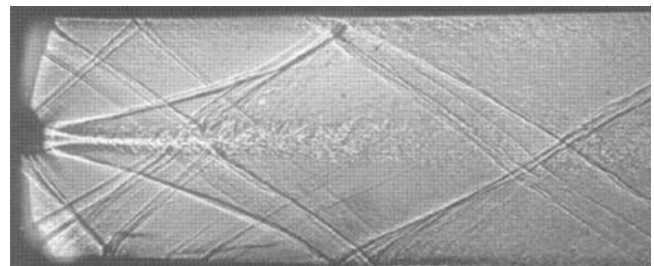


Fig.: 4 Experimental shadowgraph (Schlieren image of hydrogen injection)

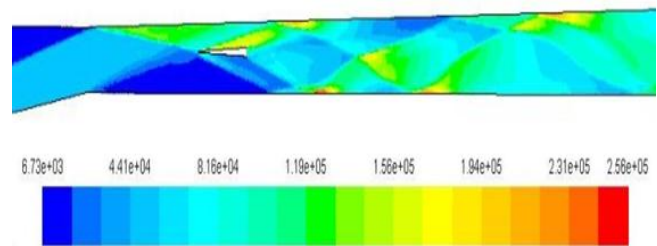


Fig.: 5 Contour plot of static pressure ( $\alpha=0^\circ$ )

Towards the combustor exit, the intensity of the shock train decreases and consequently the wall static pressure too. For the case with central injector, the first pressure peaks are produced by the shock formed at the inlet-compression ramp, and then the shock goes under the cowl and impacts 485.7mm downstream from the inlet. At the axial location  $x = 550$  mm, the combustor flow path has a small change in geometry, the upper wall deflects  $-3^\circ$  with respect to the horizontal. Here, an oblique shock is generated. This oblique shock is small in magnitude and vanishes before it reaches the central injector.

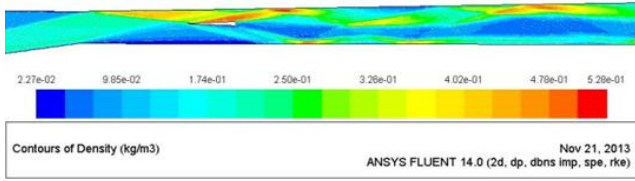


Fig.6 Contours of Density ( $\alpha=0^\circ$ )

In a supersonic stream, large non-uniformities of Mach number are possible owing to the presence of waves crossing the stream.<sup>18</sup> then, at supersonic speed, the flow field at any given section of the duct can have a wide variation of local Mach number. In the Mach number plots, the inlet-compression shock is visible. After the compression shock, the Mach number contours change from Mach = 8 to Mach (M) < 6.

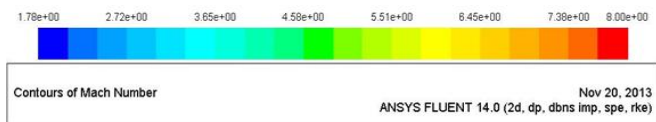
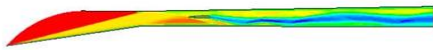


Fig.7 Contours of Mach number ( $\alpha=0^\circ$ )

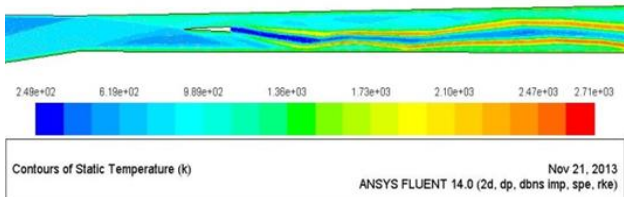


Fig.8 Contours of Static Temperature ( $\alpha=0^\circ$ )

Fig. 8 shows the temperature distribution for the angle of attack  $\alpha=0^\circ$ . The heat addition in the combustor changes both static temperature & the flow velocity. Thus it is reflected in an increase of total temperature. The chemical kinetics and chemical equilibrium of heat release depends on the static temperature.<sup>19</sup> Hydrogen is transported and mixed with the surrounding flow due to stream wise vorticity induced by lobed strut injector. After hydrogen is mixed and Pressure & Temperature are high enough for auto ignition, then combustion starts. The intensity of the vortices depends mainly on the injector's geometry.

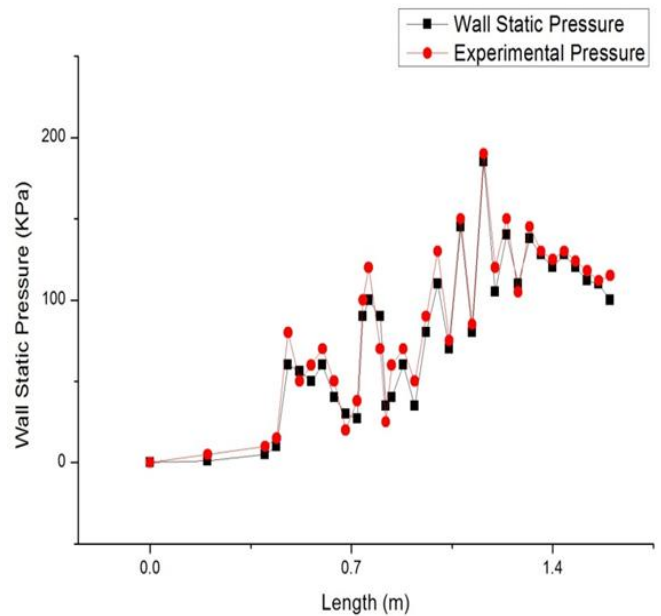


Fig.: 9 Experimental (M=8) and Numerical wall pressure distribution for  $\alpha=0^\circ$  for Mach No: 7

Fig.: 9 shows the pressure distribution at the top wall for an equivalence ratio  $\phi=1$  &  $\alpha=0^\circ$ , and Upstream from the central injector the shock pattern remains unchanged. The increase in pressure is registered when combustion takes place. The highest pressure peak at the top wall is registered at  $x \approx 1160$  mm with a corresponding pressure  $p \approx 185$  KPa.

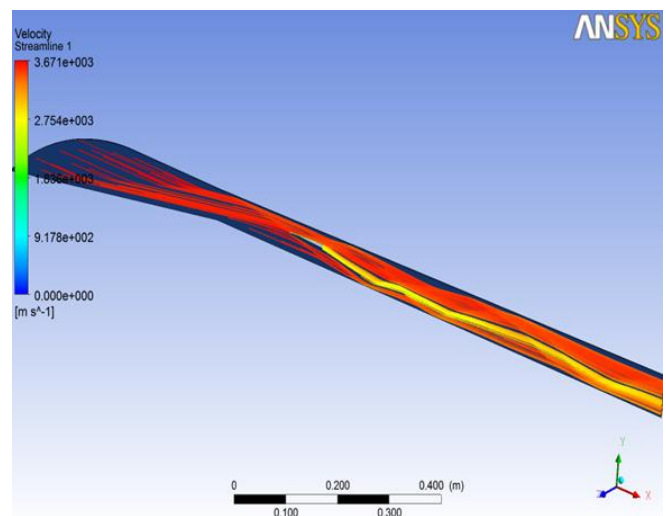


Fig: 10 Velocity streamlines

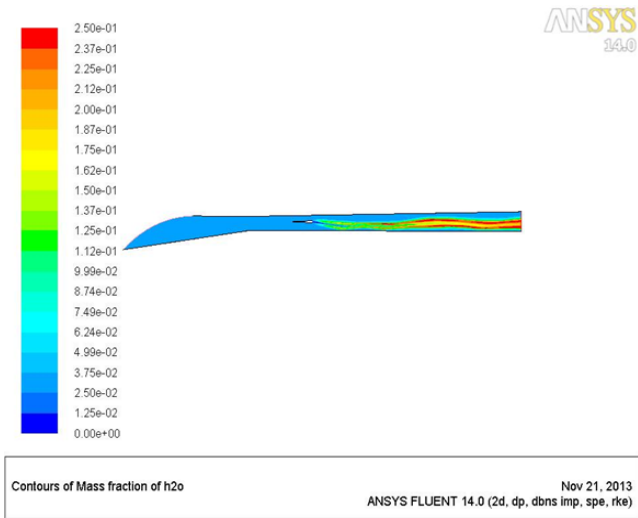


Fig: 11 Contour of mass fraction of H<sub>2</sub>O

To provide a better view of the reacting flow field, the H<sub>2</sub>O mass fraction distribution at the symmetry plane is plotted in Fig. 11. The higher distribution of Y<sub>H<sub>2</sub>O</sub> at the center of the channel shows that the flame is located mainly in the center of the combustor.

### VII. COMBUSTION EFFICIENCY

A useful parameter to identify the combustor performance is the combustion efficiency. The combustion efficiency  $\eta_{comb}$  represents how much of the hydrogen has been burned in a given cross section (Ax) with respect to the total injected hydrogen. The combustion efficiency is defined by Gerlinger<sup>16</sup> as:

$$\eta_{Comb}(X) = 1 - \frac{\int A(x) \rho_{gas} U Y_{H2} dA}{m_{H2inj}}$$

Where  $\rho$  is the gas density, Y<sub>H<sub>2</sub></sub> is the mass fraction of hydrogen, m<sub>H<sub>2</sub>inj</sub> is the injected hydrogen mass flux, and u is the velocity component normal to the cross section. The combustion efficiency is presented in Fig. no.12. The plot starts right after the trailing edge of the central injector (x = 732mm) since no hydrogen is available in upstream direction. The ignition of the fuel-air mixture takes place downstream of the trailing edge of the injector. The combustion efficiency grows near the injection region where hydrogen is rapidly mixed due to the strong stream wise vorticity. For high equivalence ratios, the combustion efficiency decreases as a consequence of the decrease in the mixing efficiency due to high values of hydrogen mass flow.<sup>1,17</sup> For the present case, the highest combustion efficiency for a stoichiometric condition ( $\phi = 1$ ) is around 78%. The high equivalence ratio and the high incoming Mach number, prevents the total mixing of the fuel and oxidizer. Combustion cannot take place until micro mixing has occurred. For  $\phi = 1$ , a large amount of hydrogen is injected and not completely mixed. Thus, the combustion efficiency decreases. The strong vorticity produced by the central lobed injector is responsible for the mixing. As the vortices travel downstream they become weak and their ability to spread the fuel into the surrounding flow decrease. This leads to a decrease in mixing and consequently in combustion efficiency.

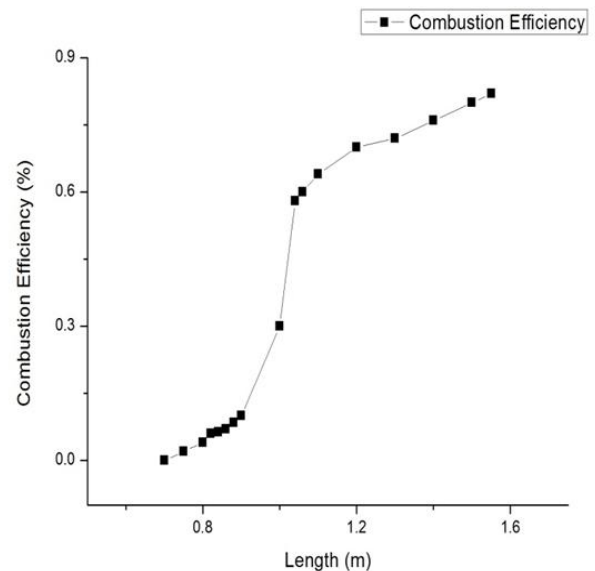
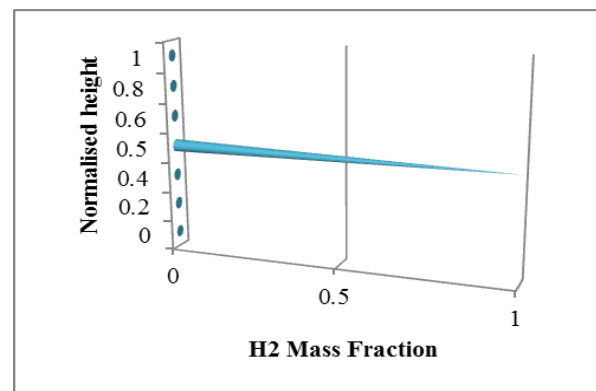
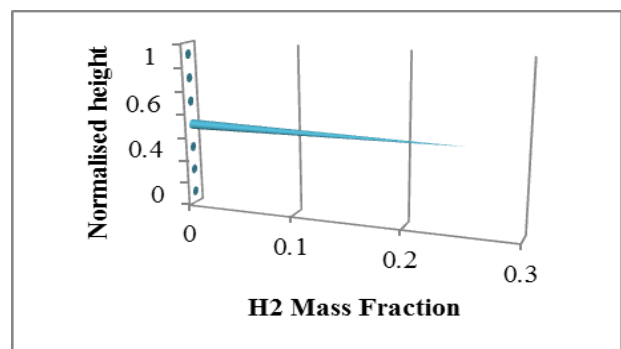


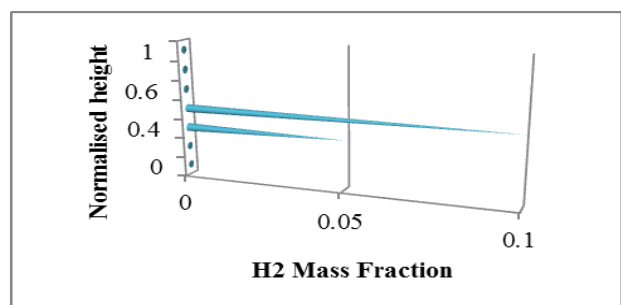
Fig. 12: Computed combustion efficiency for angle of attack  $\alpha=0^\circ$ , equivalence ratio  $\phi = 1$ .



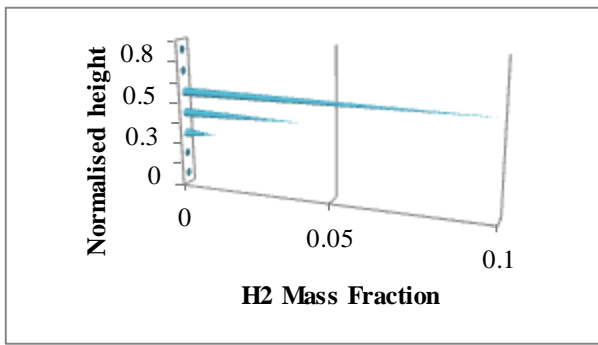
(a) X = 732.20mm



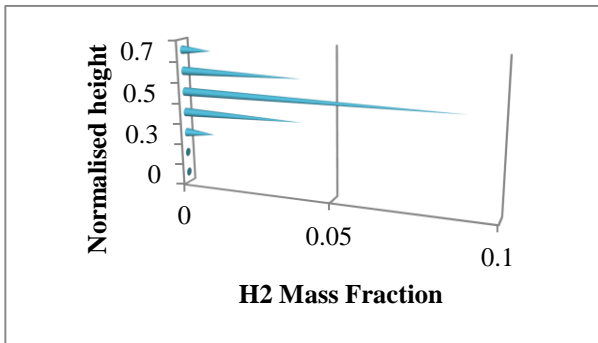
(b) X = 772.95mm



(c) X = 810.70mm



(d) X = 850.45mm



(e) X = 928.96mm

Fig. 13: Computed hydrogen mass fraction distribution  $Y_{H_2}$  for different axial locations at the symmetry plane for angle of attack  $\alpha=0^\circ$  and  $\phi = 1$ .

The distribution of the hydrogen mass fraction ( $Y_{H_2}$ ) at different axial locations is showed in Fig. 13. The height is normalized with respect to the height of the local cross section. The cross section at five different axial locations for the angle of attack  $\alpha=0^\circ$  is presented. The first axial location ( $x = 732.20\text{mm}$ ) is immediately after the hydrogen injection. In downstream direction,  $Y_{H_2}$  decreases. The decrease in  $Y_{H_2}$  indicates that mixing between fuel and oxidizer takes place. Actually the diffusion of the hydrogen into the air takes place at the center of the channel. Thus, the highest temperature flames are kept away from the walls. This mixing characteristic of the central strut injector is an advantage in comparison with the normal (wall) injection, where combustion might occur close to the walls.

The geometry of the central lobed strut injector produces strong stream wise vorticity. This vorticity leads to a mixing of the hydrogen with the main stream. The vortices formed by the lobed strut injector enhance the mixing and consequently decrease the hydrogen mass fraction in the combustor.

### VIII. CONCLUSION

In this paper, a numerical investigation of a Scramjet inlet-combustor for a flight Mach number  $M = 7$  at altitude  $h = 30\text{km}$  is presented. The flow structure through the hypersonic combustor and the interactions between the inlet and the combustor were investigated and also the numerical simulations were performed for an inlet-isolator-combustor model. For all reacting cases, a stoichiometric fuel-air

condition with an equivalence ratio  $\phi = 1$  was used. Different flow and performance parameters like static wall pressure, temperature, Mach number, and species distribution as well as combustion efficiency were discussed. No influence of the central strut injector in upstream direction towards the isolator was found. However, at the leading edge of the central strut injector, an oblique shock is produced and reflected towards the walls. This shock modifies the shock pattern in the combustor. In the reacting case with an equivalence ratio  $\phi = 1$ , no thermal choking was observed. For this configuration, the area increase in the divergent combustor is sufficient to avoid inlet instabilities.

### REFERENCES

- [1] E. Rabadan, B. Weigand. Numerical Investigation of a Hydrogen-fueled Scramjet Combustor at Flight Conditions. In: The 4th European Conference for Aerospace Sciences, St. Petersburg, Russia, 2010.
- [2] T. Nguyen. Numerical Investigations of Relaminarization in Supersonic and Hypersonic Flows. Ph.D. Dissertation, Chair for Computational Analysis of Technical Systems, RWTH Aachen University, Aachen, Germany, to be published.
- [3] Vadim Yu. Aleksandrov Alexander N. Prokhorov Vyacheslav L. Semenov "Hypersonic Technology Development Concerning High Speed Air-Breathing Engines" Proceedings of ICFD 10:Tenth International Congress of Fluid Dynamics December 16-19, 2010, Stella Di Mare Sea Club Hotel, Ain Soukhna, Red Sea, Egypt
- [4] K. A. SKINNER and R. J. STALKER "Species Measurements in a Hypersonic Hydrogen-Air, Combustion Wake"
- [5] J. SWITENBANK "HYPERSONIC AIR-BREATHING PROPULSION" Department of Fuel Technology and Chemical Engineering, University of Sheffield 2002, AIAA paper 2000-5210.
- [6] I. N. MOMTCHILOFF, E. D. TABACK, AND R. F. BUSWELL "KINETICS IN HYDROGEN-AIR FLOW SYSTEMS. I. CALCULATION OF IGNITION DELAYS FOR HYPERSONIC RAMJETS
- [7] Richard C. Oldenborg, David M. Harradine, Gary W. Loge, John L. Lyman, Garry L. Schott. and Kenneth R. Winn "CRITICAL REACTION RATES IN HYPERSONIC COMBUSTION CHEMISTRY"
- [8] S. Yungster, K. Radhakrishnan "Simulation of unsteady hypersonic combustion around projectiles in an expansion tube" Shock Waves (2001) 11: 167-177
- [9] K. Kumaran and V. Babu, "Investigation of the effect of chemistry models on the numerical predictions of the supersonic combustion of hydrogen", Combustion and Flame, vol 156, 2009, pp.826-841.
- [10] Shigeru Aso, ArifNur Hakim, Shingo Miyamoto, Kei Inoue and Yasuhiro Tani, "Fundamental study of supersonic combustion in pure air flow with use of shock tunnel", Department of Aeronautics and Astronautics, Kyushu University, Japan , Acta Astronautica, vol 57, 2005, pp.384 - 389.
- [11] S. Zakrzewski and Milton "Supersonic liquid fuel jets injected into quiescent air", International Journal of Heat and Fluid Flow, vol 25, 2004, pp.833-840.
- [12] Kyung Moo Kim 1, Seung Wook Baek and Cho Young Han, "Numerical study on supersonic combustion with cavity-based fuel injection", International Journal of Heat and Mass Transfer, vol 47,2004, pp.271-286
- [13] D. Cecere , A. Ingenito , E. Giacomazzi , L. Romagnosi , C. Bruno Hydrogen/air supersonic combustion for future hypersonic vehicles, international journal of hydrogen energy 36( 2011 ) 11969-11984.
- [14] Ghislain Tchien, Yves Burtshell, David E. Zeitoun "Numerical study of the interaction of type IVr around a double-wedge in hypersonic flow Original Research Article Computers & Fluids, Volume 50, Issue 1, November 2011, Pages 147-154
- [15] M Deepu "Recent Advances in Experimental and Numerical Analysis of Scramjet Combustor Flow Fields", Vol. 88, May 2007
- [16] P. Gerlinger, P. Stoll, M. Kindler, F. Schneider and M. Aigner. "Numerical investigation of Mixing and Combustion Enhancement in Supersonic Combustors by Strut Induced Streamwise Vorticity." In: Aerospace Science and Technology ELSEVIER, 2008, 12:159-168.
- [17] M.C. Banica, J. Chun, T. Scheuermann, B. Weigand and J. v. Wolfersdorf. "Numerical Investigation of the Performance of a Supersonic Combustion Chamber and Comparison with Experiments". In: The 6th European Symposium on Aerothermodynamics for Space Vehicles, Versailles, France, 2009.

- [18] A. Ferri. Mixing-controlled Supersonic Combustion. In: Annual Review Fluid Mechanics, 1973, 5:301-338
- [19] W. Heiser and D. Pratt. Hypersonic Airbreathing Propulsion. AIAA Education Series, Washington DC, 1994.
- [20] Weigand, U. Gaisbauer. An Overview on the Structure and work of the DFG research training group GRK 1095: Aero-thermodynamic Design of a Scramjet Propulsion System". In: 16th AIAA/DLR/DGLR International Space Planes and Hypersonic Systems and Technologies Conference, 2009.
- [21] U. Gaisbauer, B. Weigand. Structure and Results of the Research Training Group GRK 1095/2:Aero-thermodynamic Design of a Scramjet Propulsion System" an overview of the second working phase. In: International Conference on Methods of Aerophysical Research, ICMAR 2010.



**K.M.Pandey** did his PhD in Mechanical Engineering in 1994 from IIT Kanpur. He has published and presented 170 papers in International & National Conferences and Journals. Currently he is working as Professor of the Mechanical .Engineering Department, National Institute of Technology, Silchar, Assam, and India. He also served the department in the capacity of head from July 07 to 13 July 2010. He has also worked as faculty consultant in Colombo Plan Staff College, Manila,

Philippines as seconded faculty from Government of India. His research interest areas are the following: Combustion, High Speed Flows, Technical Education, Fuzzy Logic and Neural Networks , Heat Transfer, Internal Combustion Engines, Human Resource Management, Gas Dynamics and Numerical Simulations in CFD area from Commercial Software's.



**Gautam Choubey** is doing his M.Tech in Mechanical (Thermal) Engineering Department from NIT Silchar from 2012. His research interests are CFD, Combustion and Gasification